Research Article

A Complex Topological Phase in C-Spin Active Matter

Alessandro Scirè[1]

1. University of Pavia, Italy

This work unveils complex topological properties within a recent theoretical model concerning the interplay of positional and orientational order. The model features "complementary-spins" (c-spins), symbolic agents having two-dimensional spatial mobility and rotational freedom, divided into two populations with contrasting positional and orientational interactions. The model is governed by the system size and a control parameter that splits their natural rotational frequencies, a form of circular anisotropy. For a given system size and for small anisotropy, equilibrium patterns showing both positional and orientational regularity emerge, consistent with local stability predictions. For moderate anisotropy, the system develops complex topological point defects, driven by phase singularity and bistable with the uniform patterns. The defects are constituted by curled orientational textures embedding two c-spin loop trains that counter-rotate around the same center, exhibiting regular spacing, spin-momentum locking, and dissipationless flow. These emergent non-local defect complexes are extremely robust to noise and capable of self-repair, and constitute a whole new class of non-equilibrium dissipative states. These are, in fact, topological vortex states, classifiable by a two-valued topological charge. For anisotropy exceeding the local stability threshold, active turbulence (deterministic chaos) takes place and order is lost. A statistical analysis revealed the coexistence of a double phase transition at a critical parameter value: an "ordinary" symmetry-breaking transition associated with standard collective synchronization and a novel topological phase transition activating the vortex complexes. Quantitative boundaries have been evaluated, either analytically or numerically, in the parameter space. Increasing system size enhances organizational complexity, developing spin-momentum locked transport networks of increasing complexity. Thanks to its self-organizational properties, this work provides a new tool to understand robustness and morphogenesis in living systems.

 doi.org/10.32388/9ZDJVU

Corresponding author: Alessandro Scirè, alessandro.scire@unipv.it

1. Introduction

Active matter [1] is a relatively new classification in soft matter physics, defined by the presence of a large number of interacting agents that consume energy to move or exert forces. This field brings together aspects of symmetry, non-equilibrium thermodynamics, and topology [2]. The most extensively studied model in the field, the Vicsek model [3] published in 1995, deals with systems composed of self-propelled agents and demonstrates how local interactions can generate collective motion, displaying the emergence of complex phenomena and phase transitions. In general, the core interest in investigating organization patterns in non-equilibrium systems stems from their ability to exhibit complex processes like adaptation and self-organization, and scrutinizing these patterns provides information about how living and non-living systems achieve order, robustness, and dynamic functionality far from equilibrium. Topological states [4] are a promising tool in this sense, for being non-local and robust against disorder. Under certain conditions, active matter exhibits out-of-equilibrium structures that are both topological and dissipative, such as topological defects [5] and topologically protected edge modes (sound modes) [6]; this combination (topological and dissipative) can lead to unique and robust complex states that maintain their function despite energy loss, a phenomenon paralleled in emergent life forms [7].

Recently, topological phases in active matter have been found to influence the mechanics and organization of living tissues: an active nematic [8] state can emerge in epithelial cell layers, where cells collectively align and generate active forces from their internal cytoskeletons, and spontaneously generated topological defects move and annihilate in pairs. These defects, which emerge from the collective, self-organized movement of cells, serve as crucial organizing centers for biological processes. By modeling epithelial layers as active nematic liquid crystals, researchers have demonstrated that the stresses generated by these defects can dictate cell fate and drive large-scale tissue behaviors like extrusion, migration, and morphogenesis [9]. In the Hydra organism, the precise arrangement of topological defects is utilized to position its limbs, mouth, and foot [10].

Aside from the aspects concerning active nematics (mostly developed in the frame of the modified Navier-Stokes Equation), understanding how self-propelled units coordinate their movement, orientation, or internal oscillations to produce coherent large-scale behavior also falls within the frame of collective synchronization. Arthur Winfree pioneered the use of mathematical models to describe

biological clocks, non-equilibrium systems that consume energy (ATP) to maintain rhythm and synchronize with environmental cues. His Winfree model [11] provided an early, complex framework for synchronizing diverse oscillators, influencing Yoshiki Kuramoto, who developed the more analytically tractable Kuramoto model [12] establishing the foundational theories for collective synchronization in biological systems. The transition to synchronization in the Kuramoto model is a classic example of a spontaneous symmetry-breaking phase transition in a non-equilibrium system. However, the Kuramoto model can be modified to exhibit a topological phase transition: When it is placed on a spatial lattice (like a two-dimensional grid), the relative positioning is fixed, but the spatial pattern of the synchronized phases exhibits features of positional/topological order related to the Berezinskii-Kosterlitz-Thouless transition and defect binding [13].

However, the (highly successful) Kuramoto model – including its numerous variations [14] – describes the synchronization of phases or internal states, not the collective motility characteristic of active matter agents. The standard Kuramoto model and most of its traditional variations deal only with orientational order (phase synchronization); it focuses on the internal phases of oscillators at fixed spatial locations, without explicitly modeling their physical motion in space.

A significant recent variation called the 'swarmalator' [15] model explicitly links the internal Kuramoto phase dynamics to the physical spatial position dynamics of mobile agents. These models exhibit coupled phase and spatial order, such as states where particles cluster in space and synchronize their phase simultaneously. In specific theoretical variations, particularly in the hydrodynamic (continuum) limit or models with non-reciprocal forces, swarmalator models exhibit states of a topological nature [16].

However, despite exciting progress in connecting collective synchronization to symmetry-breaking and topological phase transitions, significant aspects of topological protection in space-time synchronization of mobile agents remain largely unexplored. In the absence of a general theory, research relies on the creation of new paradigms.

This work contains a numerical analysis of the organizational properties of a recently introduced [17] [18] theoretical model for the interplay of positional and orientational (phase) order. The model consists of many symbolic spin agents able to rotate and move in 2D, and divided into two subpopulations. These spins interact in a complementary scheme: when belonging to the same population, spins repel each other positionally and attract orientationally; when belonging to different populations, they do the opposite. Hence, the two spin subpopulations interact in a complementary way, so I have named these

units *complementary-spins* or *c-spins* for short. The interaction decays with distance. The system is given two parameters, the total number of elements (equally divided between the two populations) and a control parameter that splits the natural rotational frequencies of the two populations and induces a locking-to-unlocking phase transition. Also, the control parameter makes the system active, i.e., makes the units capable of orientational motion, which, due to variable coupling, translates to spatial self-propulsion.

The numerical analysis of collective behaviors reveals that, under certain conditions, robust monopole-vortex complexes emerge. These complexes can be classified as topological dissipative structures, exhibiting properties characteristic of a topological phase, including non-locality, robustness, effective dissipationless transport, and spin-momentum locking. The system displays the coexistence of two phase transitions at the same critical parameter value: an ordinary symmetry-breaking transition associated with collective synchronization and a novel topological phase transition that activates the monopole-vortex complexes. I have investigated these phase transitions using collective parameters and derived analytical formulas (either by calculation or by numerical fitting) to generate a first portrait of the phase diagram in the parameter space.

When the system size is increased, the collective organization shows a significant increment of complexity: the single vortex appearing in small systems is replaced by a flexible morphogenetic flow that generates dynamic compartments, connecting this work with previous findings [17][18]. Many different scenarios unfold at that point, which will be the subject of future research.

The manuscript is organized as follows: Section 2 describes the complementarity model in the new c-spin representation. Section 3 presents the main findings of this work, subdivided into four subsections: Subsection 3.1 provides a simple derivation of the threshold value of the control parameter for the order-disorder transition. Subsection 3.2 first presents examples of possible collective dynamics for a small, but statistically significant, ensemble, and then focuses on the statistical properties as the control parameter is varied from below to above the threshold. Subsection 3.3 discusses the phase diagram in the parameter plane N vs. Δ. Subsection 3.4 provides illustrative examples and comments concerning the complex collective dynamics that occur in larger systems. Section 4, the Discussion, is dedicated to summarizing and concluding the manuscript, emphasizing the reasons for interest in this work.

2. The Complementarity Model in the c-spin representation

The model under analysis has already been considered in preliminary works [17][18]. It consists of many agents endowed with spatial (2D) and rotational degrees of freedom; the agents are thus able to move and rotate, and they are divided into two subpopulations. Differently from previous publications [17][18][19], in this work each population is represented by a distinct color (blue and red), and the positional/rotational dynamics is represented by symbolic spins. The system is thus depicted as many two-color rotating arrows moving in a plane, as sketched in Fig. 1, panel (a). This representation proved more effective than the previous one for visualizing the morphology of the emerging orientational patterns (defects) and waves, as further elucidated in the manuscript.

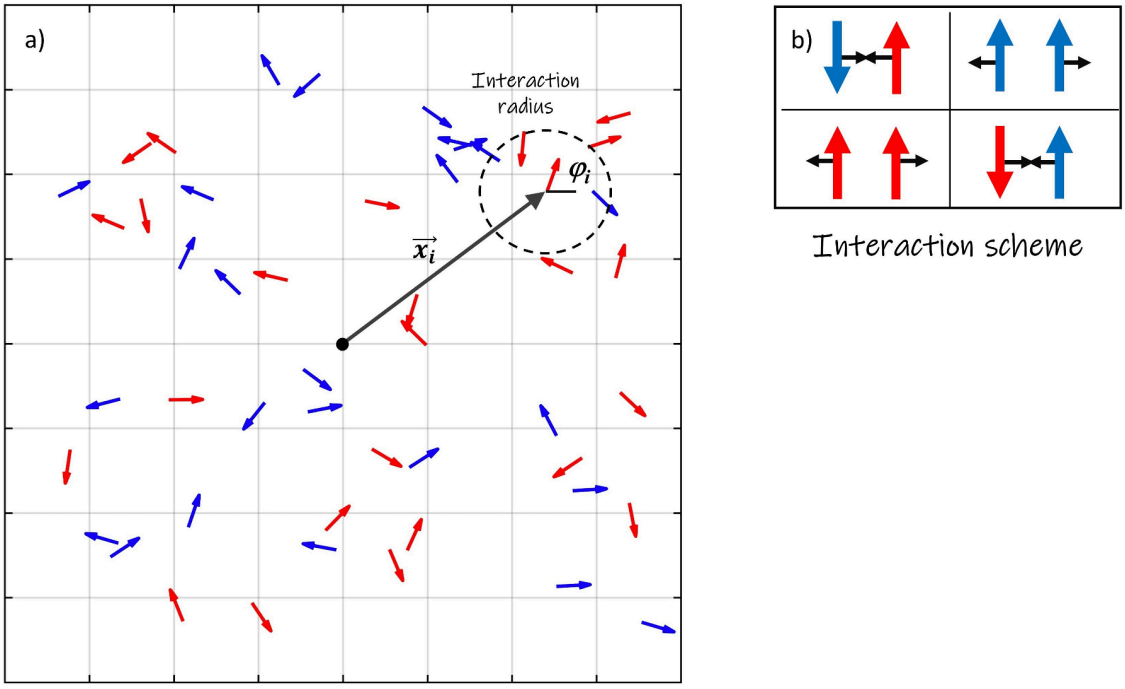

Figure 1. Sketch of the Complementary-Spin Model. a) The model assigns both a position and an angle in [0,2π] to each spin. b) Interaction forces are complementary based on color: same-colored spins repel positionally and attract orientationally, while different-colored spins do the opposite. All interaction strengths decrease with increasing positional distance.

Each spin is given a positional ($\vec{\mathbf{x}}_i$) and an angular/orientational (φ_i) degree of freedom in [0,2π], with $i = 1...N$, where N is the total number of spins. I assume as many blue spins as red ones. These spins interact by a *complementary scheme* as sketched in Fig. 1, panel (b), i.e., spins of the same color repel positionally

doi.org/10.32388/9ZDJVU

and attract orientationally, whereas spins of different colors do the opposite. The interaction strength decays with the positional distance; hence, it is a short-range interaction model.

The equations of motion for each *i-th* spin are

$$\begin{cases} \dot{\vec{x}}_i = \sum_{j=1}^{N} \nabla_i \, W\left(\left|\vec{x}_i - \vec{x}_j\right|\right) \cos(\varphi_i - \varphi_j), & (1) \\ \dot{\varphi}_i = \gamma_i \Delta + \sum_{j=1}^{N} \gamma_i \gamma_j \, W\left(\left|\vec{x}_i - \vec{x}_j\right|\right) \sin(\varphi_i - \varphi_j), & (2) \end{cases}$$

where ∇_i means differentiation with respect to the *i-th* direction, $\vec{x}_i$ and φ_i are respectively the spatial (in $\mathbb{R}^2$) and angular (in S^1) coordinates of the *i-th* unit, *i = 1,...N*, and $|\vec{x}_i - \vec{x}_j|$ is the Euclidean distance in $\mathbb{R}^2$. Since the system (1)-(2) is based on a complementary type of interaction, I have named the two-type units of the system *c-spins* (meaning complementary-spins). The functional wells (that make the interactions *local* with characteristic length L = 1) are chosen as exponential:

$$W\left(\left|\vec{x}_i - \vec{x}_j\right|\right) = -e^{-\left|\vec{x}_i - \vec{x}_j\right|^2}. \quad (3)$$

The specific choice of an exponential decay does not qualitatively affect the results. The two-valued coefficients γ_i define the *i-th* oscillator color; i.e., γ_i = +1 if the oscillator is red or γ_i = –1 if it is blue. Mathematically, model (1)–(2) is a many-body dissipative and nonlinear dynamical system, and Δ is a control parameter. The effect of Δ in Eq. (2) is to split the natural frequencies of red and blue spins, giving each spin a rotational speed term that is clockwise for red spins and counterclockwise for blue spins; in a physical system, Δ would be called a *circular anisotropy*, hence I will often refer to Δ as 'anisotropy' in the rest of the manuscript. Collectively, the parameter Δ triggers an order-to-disorder phase transition in the system upon overcoming a specific locking/unlocking threshold, driving the system to deterministic chaos. The parameter Δ, in fact, makes the system *active* because it provides the spins with a phase drift which, due to variable coupling, can indirectly activate positional dynamics. The term $\cos(\phi_i - \phi_j)$ acts as "spin-orbit" coupling—it links the spatial motion to the internal orientation state; this is crucial for topological structure formation, as elucidated further in the manuscript. The $\sin(\phi_i - \phi_j)$ term acts as the synchronization torque, a hallmark of the Kuramoto model.

3. Results

3.1. Dipolar solutions and local instability threshold

According to the interaction scheme reported in panel (b) of Fig. 1, the c-spins tend to organize in antiparallel pairs of red-blue spins (I have named these pairs c-dipoles), i.e., forming an angle $\phi = \pi$, locked in relative orientation and relative position. This is strictly true only when $\Delta = 0$; in fact, from (1)–(2) it can be shown that the relative angle ϕ between two c-spins in a c-dipole (far from other interactions) satisfies the following equation:

$$\dot{\varphi} = 2\Delta + \sin\varphi, \tag{4}$$

i.e., the well-known Adler equation [20], which is closely related to the individual oscillator dynamics within the broader Kuramoto model framework discussed earlier. The locking threshold is $\Delta_{th} = ½$; below this threshold—which determines a local transition from stable to unstable dynamics as pictured in Fig. 2—the two c-spins are locked to the same spatial position and to a relative angle equal to

$$\varphi = \pi - \arcsin(2\Delta), \tag{5}$$

that reverts to $\phi = \pi$ when $\Delta = 0$. If $|\Delta| > ½$, the two c-spins unlock via a saddle-node bifurcation and display a dynamic state in both position and orientation. Without loss of generality, in the following, I will consider positive values for Δ.

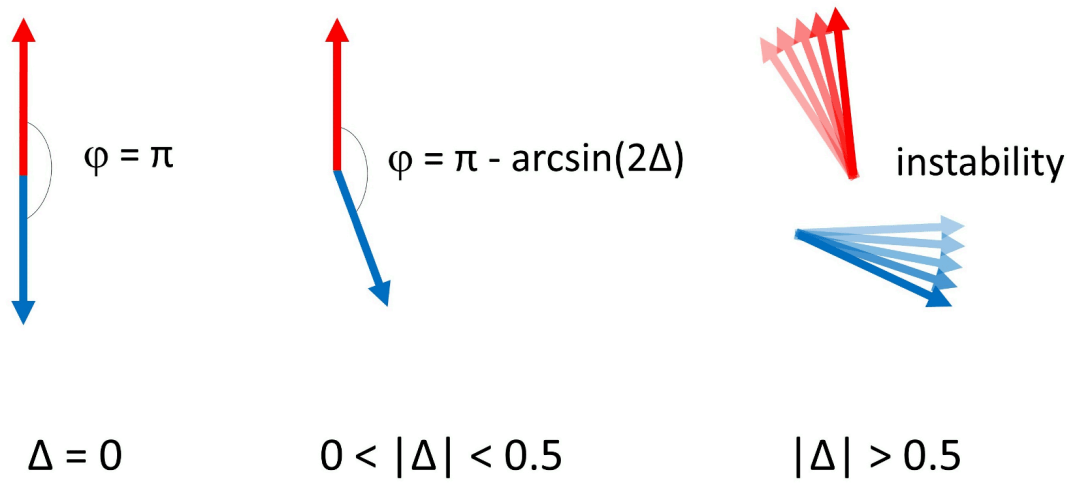

Figure 2. Illustrates the phase dynamics and locking behavior of a c-dipole. C-spins typically form antiparallel pairs called c-dipoles, which align at an angle of π when the detuning parameter Δ=0. The Adler equation, which governs oscillator locking, describes the orientation and position of these pairs and predicts a locking threshold at Δ_{th} = ½. Below the threshold, the c-spins are phase-locked at a specific relative angle; above the threshold, they unlock through a saddle-node bifurcation and become dynamic.

3.2. Collective behavior of a small ensemble

In this subsection, I report on numerical simulations concerning an ensemble of N = 80 c-spins for increasing values of the control parameter Δ.

Weak anisotropy

I have numerically integrated, by means of a standard method, Eqs. (1)–(2) for N = 80 c-spins with Δ = 0.1, i.e., well inside the stable locking range Δ < ½. The initial conditions are random spin angles with a uniform distribution between 0 and 2π and random spin positions uniformly distributed in a square box; the size of the box is chosen so that, statistically, each spin sees at least one other spin within its interaction radius, i.e., the box side is equal to $\sqrt{N}$ so that the c-spin density inside the box is equal to 1. The resulting spatiotemporal dynamics is shown in Movie S1, and the regime configuration is reported in Fig. 3.

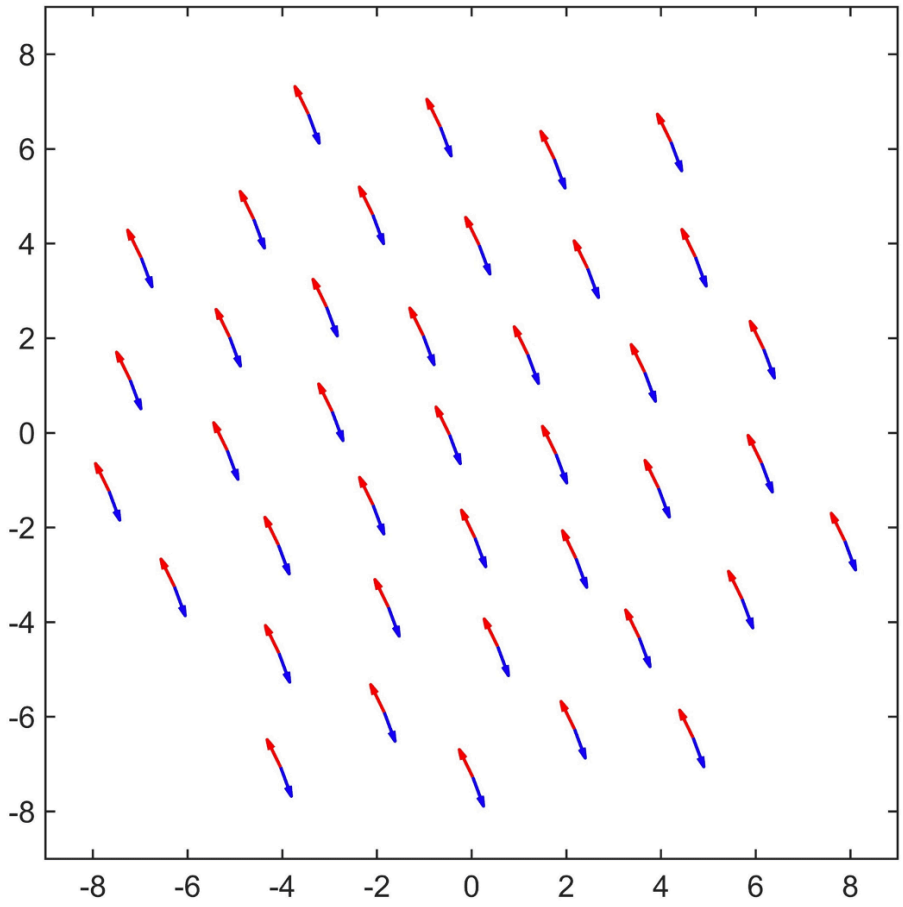

Figure 3. A type ① solution: a pattern of c-dipoles possessing both positional and orientational order. This pattern represents an equilibrium state resulting from the spontaneous breaking of continuous circular symmetry, where c-dipoles are aligned at a specific angle, randomly determined by initial conditions.

The pattern reported in Fig. 3 is made of (quasi) regularly spaced c-dipoles, each of which fulfills the local stability properties of the single c-dipole (see Fig. 2b). The pattern of Fig. 3 represents an equilibrium state associated with the spontaneous breaking of a continuous circular symmetry; like in ferromagnetic systems or in collective synchronization, the c-dipoles are forced to align at a specific angle, randomly determined by the initial conditions. This kind of pattern is referred to hereafter as a Type ① solution. The spatial regularity is due to a weak repulsive dipole-dipole force, which is proportional to Δ^2 and pushes the pattern to expand. The expansion rate is logarithmic; consequently, for practical purposes, it vanishes when it attains approximately three times the interaction length.

doi.org/10.32388/9ZDJVU

Moderate anisotropy

Increasing Δ, without crossing the local stability threshold, a different collective behavior shows up, bistable with type ①. The Movie S2 shows the spatiotemporal evolution of N = 80 c-spins with Δ = 0.2. After the transient has expired, the movie shows the appearance of a topological *vortex* exhibiting a peculiar twofold structure: a static texture, where the c-dipoles curl around a central core, surrounding a dynamic state made of two positional and orientational trains of equidistant counterpropagating c-spins that insist on the same loop trajectory. The distance between adjacent c-spins of the same color in the loop is equal to 1 with very small deviation; the orientational and positional motions are synchronized in a Spin-Momentum locked state, i.e., one full rotation in spin corresponds to a full rotation in the space loop. Surprisingly, the red and blue c-spin trains slide over each other "frictionlessly," despite the value of Δ (smaller than the locking threshold) would require that c-spins of different colors attract and lock in the same position. I have called that vortex complex (static texture + dynamic loop) a *type* ② solution.

To convey the information contained in the movie as much as possible in a single figure, I have generated a picture taken from Movie S2, concerning the regime situation, by superimposing frames over time. The result is similar to what happens in a photograph with a long exposure time, i.e., things that move leave a trail while things that are still stay the same, and is shown in Fig. 4a. Figure 4a depicts rotational dynamics around a central singularity, a complex point defect composed of an orientational texture and a loop flow around the singularity.

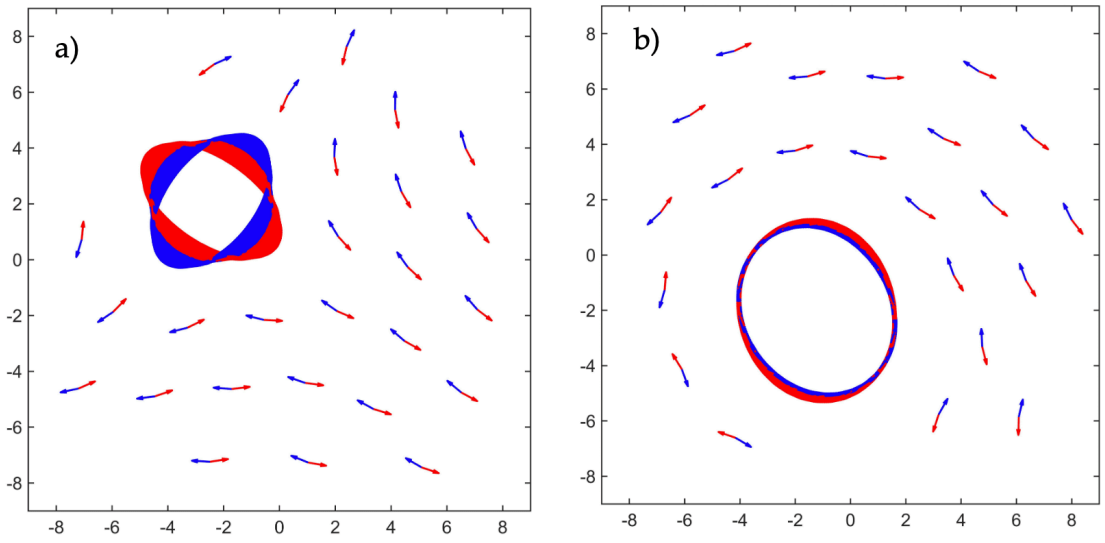

Figure 4. Illustrates persistent features state by superimposing video frames over time for N = 80 and Δ = 0.2. (a) A stable c-vortex complex with a topological charge Q = -1; (b) A stable c-vortex complex featuring a monopole with topological charge Q = 1 emerging for the same parameter values.

The winding number (or topological charge, Q) provides a quantitative measure of how many full rotations the orientation of the discrete polar units (the c-dipoles) completes when traversing a closed path around a specific point in space. This value effectively characterizes the chirality and net circulation of the static dipole pattern. A non-zero winding number indicates the presence of a stable, vortex-like rotational configuration within the texture. The quantity Q measures the net "rotation" of the static c-dipole textures when moving in a counterclockwise (CCW) closed path around the center; in particular, Q = +1 if the units rotate once clockwise (CW) around the center as in Fig. 4b, and the texture is classified as a *vortex* and the units here are the c-dipoles; whereas Q = -1 if the units rotate once CCW around the center as in Fig. 4a, and the texture is classified as an *antivortex*.

Inside the c-dipole texture, the intertwined red and blue “ribbon” represents a dynamic state made of two counter-rotating c-spin loop trains of dissipationless (also called *ballistic*) transport and has the spin rotation locked to the momentum (velocity) rotation in the plane, i.e., when a c-spin completes one loop in position, it completes a loop in orientation too, meaning the positional and orientational motions are coordinated and synchronized. This kind of behavior is a topological effect where the rotational motion is intrinsically coupled and locked to the direction of linear motion; these states are called *spin-momentum locked states*. The spin-momentum locking associated with the vortices requires careful

doi.org/10.32388/9ZDJVU

consideration, drawing an analogy with condensed matter physics. In topological materials, a fundamental spin-momentum locked state exists where an electron's momentum is intrinsically coupled to its spin orientation due to strong spin-orbit coupling [21][22]. This effect constrains the spin vector to follow a specific path as the electron moves spatially, enabling robust, dissipationless current flow along surfaces. The topological invariant in such systems is typically a winding number that quantifies how often the spin vector winds around a central point as the electron completes a loop in momentum space. In analogy with these considerations, and despite the difference in thematic area, I adapt this concept to characterize the transport loops using a relative winding number ratio:

$$W_R = \frac{\sum_{i=1}^{N} \vartheta_i\left(t - T_1\right) - \vartheta_i\left(t - T_2\right)}{\sum_{i=1}^{N} \varphi_i\left(t - T_1\right) - \varphi_i\left(t - T_2\right)}, \tag{6}$$

with $T_2 \gg T_1$. The quantity W_R is a relative winding number, which computes the ratio of the angular rotation of the spatial velocity (ϑ) with respect to the spin rotation, averaged over the ensemble. Numerical checks consistently showed that W_R is two-valued: W_R = Q = 1 for a vortex case (as in Fig. 4b), and W_R = Q = -1 for the anti-vortex case (as in Fig. 4a). The topological charge (concerning the static texture) and the winding number ratio W_R (concerning the transport loop) end up having the same value because the two structures are intimately related to each other.

Diversity of attractors and topological invariants

The attractors emerging from repeated simulations show a high degree of diversity (see Fig. 5) but can still be ascribed to one of three distinct types based on their topological properties: type ① solutions (equilibrium states with Q = 0), type ② vortex (Fig. 5a, d, and e) with Q = 1, or type ② antivortex (Fig. 5b and f) with Q = -1. The type ② solutions display a high degree of variability in terms of the number of elements involved in the internal loop; the phase singularity position in the plane; the vorticity and the velocity of the transport motion (momentum); and the spin rotation velocity in the loops. The loops always contain the core of the defect, which is “empty,” i.e., no c-spins persist inside the core. This is because the center of the defect is a phase singularity where the c-dipole orientation is ill-defined, so—as in circular optical solitons—the core is “dark.” Rarely, a double loop with a daughter loop branching off from the main formation (see Fig. 5d) appears, providing evidence of the system's capacity for morphological complexity, as discussed in a later section; however, even that “strange” configuration belongs to the Q = 1 topological class. Despite the high diversity of attractors and the complexity of the spatial arrangements, the emergent patterns can be classified by a single topological invariant.

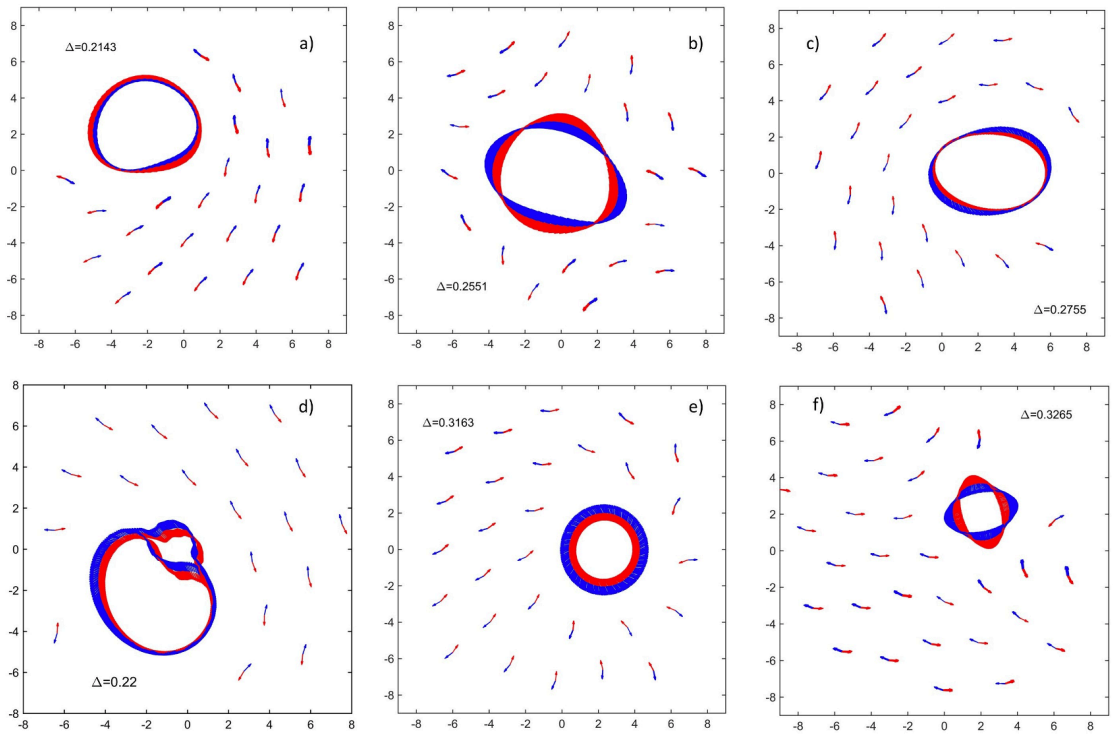

Figure 5. Illustrates the diversity of emerging attractors obtained from repeated numerical simulations using different values of $\Delta < \Delta_{th}$, N = 80. The system exhibits multistability, settling into either equilibrium type ① solutions or type ② solutions, which include both vortices (panels a, d, e) and antivortices (panels b, f) complexes. Type ② solutions display high variability in the number of elements, position, vorticity, momentum and spin velocity. A notable feature is the "dark" or empty core of the defects, which is a phase singularity where orientation is ill-defined. Rare exceptions are of the form reported in panel d.

Above the locking threshold, numerical simulations for $\Delta > ½$ show spatiotemporal chaotic dynamics in both position and orientation, a form of active turbulence, which is a global consequence of the local unlocking transition. I call these kinds of supercritical patterns type ③. Increasing Δ further, the behavior becomes more erratic, and finally, no trace of order is left.

Robustness against perturbations

The primary implication of a topological invariant is robustness. In a topological state, the value of the invariant remains unchanged under continuous deformations, minor perturbations, or a high degree of diversity in spatial arrangements. In fact, the complementary regime structures obtained in the previous subsection, made of vortex and antivortex complexes, proved to be highly resilient with respect to

doi.org/10.32388/9ZDJVU

different kinds of perturbations. First, the structures persist stably under the addition of Langevin white noise terms to Eqs. (1)–(2) even at high levels of noise. Second, I perturbed the structure in the following way: after the structure was formed, I removed one red spin from a c-dipole forming the external texture and placed it into the vortex, close to the center; the result is reported in Movie S3. The displaced element is quickly absorbed in the vortex and, after a short time, a red spin is expelled from the vortex so that it can couple back with the blue spin left uncoupled and reform a c-dipole to restore the original topology. This observed self-repairing capability is a direct consequence of the non-local topological protection inherent to these complexes [4][5].

The reported results suggest that a relatively small ensemble of N=80 c-spins shows a rich multi-stable scenario that requires a systematic analysis. Moreover, the type ② patterns are non-local solutions that cannot be understood in terms of a local stability analysis; they are therefore hard to tackle analytically moving from Eqs. (1)–(2), so I have relied on a statistical analysis based on extensive numerical simulations.

3.3. Statistical analysis

Considering the system (1)–(2), I have performed reiterated numerical simulations with Δ spanning from 0 to 1, with different realizations for each value of Δ, starting from random initial conditions with the same statistical properties: random positions in a box with a spin density equal to 1 and uniform random orientations in $[0,2\pi]$. I have taken as a reference a collective parameter: the total time-averaged kinetic energy T_{av}

$$T_{av} = \left\langle \frac{1}{N} \sum_{i=1}^{N} \dot{x}_i^2 \right\rangle, \tag{8}$$

that accounts for spatial fluctuations; $\langle \bullet \rangle$ stands for the temporal average. The results for T_{av} versus Δ are shown in Fig. 6a.

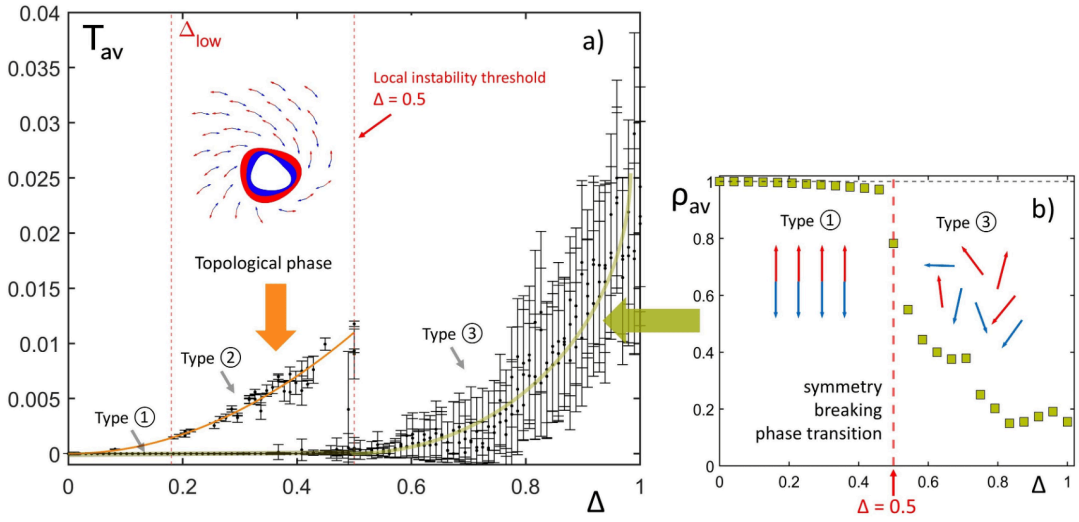

Figure 6. Panel (a) shows the time-averaged kinetic energy T_{av} as a function of the control parameter Δ. The plot reveals distinct behavioral regimes: a small Δ regime (type ① patterns) with vanishing T_{av}; a bistable intermediate regime $\Delta_{low} < \Delta < \Delta_{th}$ ($\Delta_{th} = 0.5$ is the locking instability threshold) featuring a lower branch of type ① patterns and an upper branch of type ② patterns (example in the inset); and a supercritical turbulent, chaotic regime $\Delta > \Delta_{th}$ where all order is lost. Panel (b) displays the time-averaged absolute value of the Kuramoto order parameter (ρ_{av}) as a function of Δ. The panel illustrates a Kuramoto-like phase transition behavior, specifically the transition from type ① (synchronization, $\rho_{av} = 1$) to type ③ (desynchronization/turbulence, $\rho_{av} \to 0$), obtained from initial conditions near the type ① basin of attraction.

Panel (a) of Fig. 6 shows $T_{av} \approx 0$ for low values of Δ, approximately $0 < \Delta < \Delta_{low}$ with $\Delta_{low} \approx 0.18$. In this region, the equilibrium type ① patterns, such as the one reported in Fig. 3, appear stably. For $\Delta_{low} < \Delta < \Delta_{th}$, the values of T_{av} separate into two branches. The lower branch is a continuation of the type ① patterns from the previous interval and is bistable with a second branch containing the twofold type ② patterns discussed in the previous subsection. The upper branch follows approximately a Δ^2 dependence (orange fitting line in Fig. 6a) and contains an infinite number of different attractors, separated into two families of defects: vortices and anti-vortices, associated with a topological phase transition and classified via either W_R or Q. For $\Delta > \Delta_{th} = ½$, local instability takes place, as predicted by Eq. (4); all the c-dipoles unlock, destroying both type ① and ② attractors, and chaotic dynamics appear, becoming increasingly turbulent as Δ increases further. Shortly after Δ_{th}, small vortices may still be present,

doi.org/10.32388/9ZDJVU

together with other dynamic patterns and floating spins, whereas for high values of Δ, any trace of positional and orientational order is finally lost.

The transition from type ① to type ③ patterns is understood in terms of the breaking of a local continuous symmetry; using an expression dear to complex systems, type ① to type ③ patterns are *the sum of the parts*, parallel to the melting of a crystal, to the transition to a ferromagnetic state, or to the Kuramoto phase transition to collective synchronization. It is a spontaneous symmetry-breaking phase transition of the Landau type. Indeed, it can be classified by means of the Kuramoto order parameter, modified as in previous works [17][18][19]

$$\rho e^{i\theta} = \frac{1}{N}\sum_{k=1}^{N}\gamma_k e^{i\varphi_k}. \tag{9}$$

The time-averaged absolute value $\rho_{av} = \langle\rho\rangle$ is bounded between 0 and 1, where 1 means total phase synchronization and 0 means total phase desynchronization. Panel (b) of Fig. 6 shows the typical Kuramoto-like phase transition behavior when ρ_{av} is computed versus Δ. Fig. 6b concerns the transition from type ① to type ③, obtained by making the system start from initial conditions close to the basin of attraction of the type ① solution.

It is worth noting that the point $\Delta = \Delta_{th}$ marks a double phase transition, a Kuramoto-like and a topological one. As already mentioned, the emergence of type ② attractors is not related to a spontaneous symmetry breaking of a local symmetry; it displays the characteristic features of a topological phase. Such features are the robustness and the non-local character, the topological invariants, the dissipationless transport, and the spin-momentum locking. These type ② patterns contain features surprisingly parallel to those of quantum states of matter. Specifically, the patterns exhibit features that parallel the spin helical transport regime found in topological insulators, showcasing robust, counterpropagating, dissipationless flow, found here, within a dynamical non-equilibrium system, for the first time to the best of our knowledge. However, along with similarities with other systems, the c-spin model also shows consistent peculiarities. In particular, the scenario grows increasingly complex and peculiar when more c-spins are considered.

3.4. Larger systems

In this subsection, the evolution of type ② solutions is examined as the system size N increases by means of a few examples. As a general remark, the single vortex/antivortex patterns observed in smaller systems are replaced by a flexible, morphogenetic flow that generates dynamic compartments and a progressively

more intricate positional and orientational flow as N increases. Figure 7 illustrates the progression from N=200 (simple figure-eight shape) to N=500 (more convoluted boundary loops) to N=1000 (highly intricate, compartmentalized network). A detailed analysis of the N = 1000, Δ=0.01 case is provided in reference [18]; Movie S4 shows the regime solution for N = 500 and Δ = 0.1. The c-dipoles' static texture is an antivortex with Q = -1, but the counterpropagating dissipationless currents form an intertwined phase, mixed with the c-dipole texture, i.e., the spin-momentum flow percolates the whole system size. It is still a spin-momentum locked loop structure, but more complex; calculating W_R in this case does not provide clear results, as the spin-momentum relationship is more intricate with respect to the simple 1:1 locking displayed by small systems. However, the global pattern displays both long-range order and topological protection.

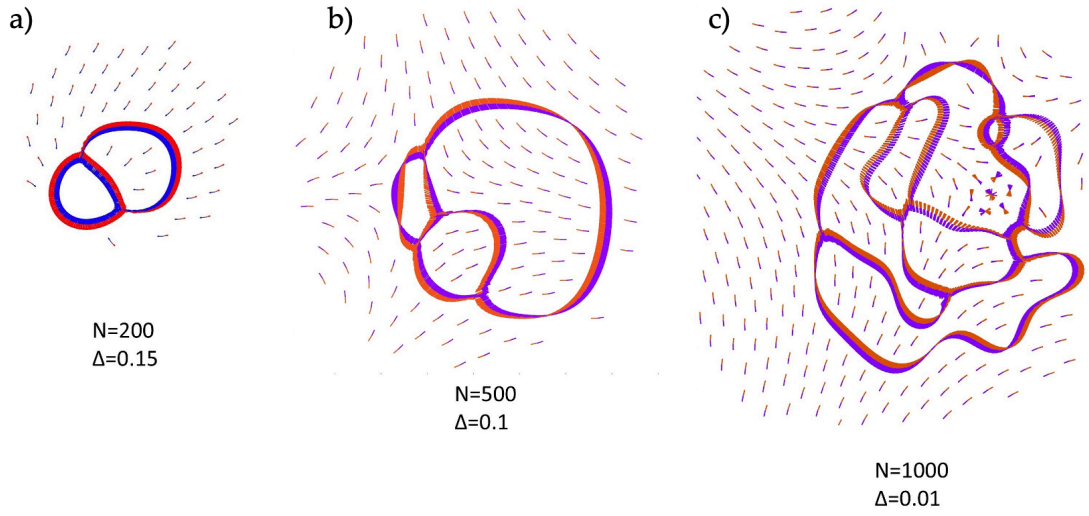

Figure 7. Sketch illustrating the increase in complexity of type ② solutions as system size N increases. The single vortex observed in small systems is replaced by a progressively complex, morphogenetic flow that forms dynamic compartments and an intricate transport network (right). This configuration represents an intertwined phase exhibiting both long-range positional/orientational order and protected topological order.

The individual c-spins that travel along the loops occupy the loops themselves in a non-regular (chaotic) fashion, while the collective flow is orderly and regular. It is a form of emergence, where the behavior of the system as a whole is different from the behavior of its individual parts. The units are chaotic at the microscale, whereas the whole system displays predictable behavior at the macroscale. This aspect

becomes more relevant for bigger structures with many further loops created by connected vortices, where the efficient routing of dynamic flow within increasingly complex network topologies becomes more complex accordingly.

The large sizes are numerically hard to tackle; the flow stabilizes after a long, non-exponential “glassy” transient with a power-law frequency spectrum [18]. Many scenarios open up that will be the object of future research.

3.3. Phase diagram

By exploring different system sizes, ranging from N = 80 to N = 1000, I have observed that the values of Δ required to obtain Type ② solutions decrease as the system size N increases. To highlight the transition between the stability region of type ① and the bistable region containing both type ① and ②, I performed extensive numerical simulations across the (N, Δ) parameter plane. The result is reported in Fig. 8, where white dots indicate the presence of a type ① uniform solution and black dots denote the emergence of type ② complexes. The analysis reveals that as N increases, the transition value of Δ (previously termed Δ_{low}) decreases following the empirical scaling relationship

$$\Delta_{low}(N) = \frac{a}{N}, \tag{10}$$

with a being a fitting parameter. Repeated simulations consistently yielded similar results, and data from single runs at higher values of N remained consistent with the scaling behavior described by Eq. (10). As an addendum to previous results, what was called “network death” in [18] can be understood in the light of Eq. (10). In [18], the emergence of a complex spin-momentum locked network with N = 1000 and Δ = 0.01 (sketched here in the c-spin representation in Fig. 7c) was reported. The network was revealed not to be stable in the very long run. In fact, Eq. (10) gives Δ_{low}(N=1000) = 0.012 as the lower stability threshold for these kinds of solutions, so, being close to the threshold but outside of it, the network was marginally stable and did not endure.

Since the density is fixed, N (the number of c-spins) also represents the area of the squared box where the dynamics initiate (see inset in Fig. 8). Consequently, the significant value is the product of the anisotropy Δ and the system size N. This product $N\Delta_{low}$ effectively acts as a minimum 'quantum' necessary to assist the formation of the topological phase, and, since Δ cannot exceed Δ_{th}= 0.5, which would activate chaotic behavior, the minimum size for having vortex/antivortex complexes is N = 24.

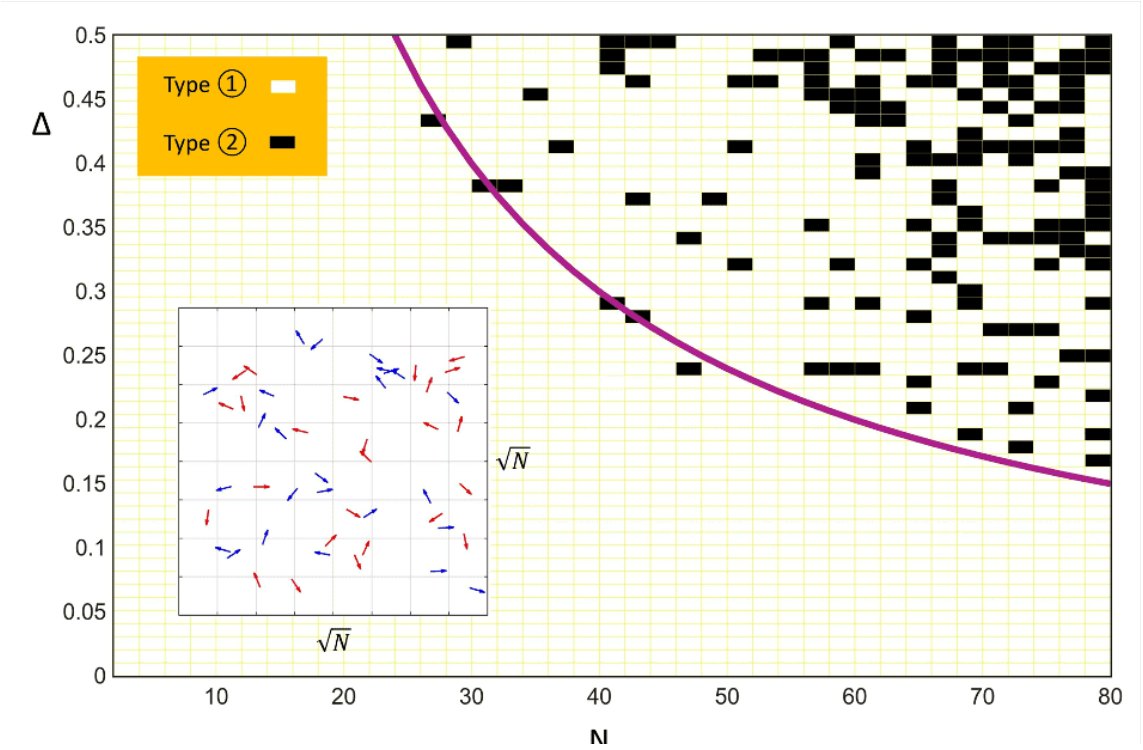

Figure 8. Phase diagram in the (N, Δ) parameter space, illustrating the transition between different solution types. White dots indicate regions where stable type ① uniform solutions appeared, while black dots denote the emergence of type ② monopole-vortex complexes. The boundary value Δ_{low} is fitted with $\Delta_{low}(N) = \frac{a}{N}$ (purple curve); a = 12.

The number N = 24 appears to be the smallest number of c-spins that can structurally support the complex arrangement required for a stable, self-organized vortex or antivortex composite; it represents the point where the behavior transitions from single-unit interactions to collective organization: the onset of collective behavior. Below N = 24, the local interactions dominate, and complex collective structures cannot "nucleate" effectively.

4. Discussion

The introduced model offers a novel framework for investigating the reciprocal effects of synchronization dynamics and physical space organization. This model features two populations of symbolic agents, termed complementary-spins (c-spins), which exhibit antagonistic positional and orientational interactions, introducing crucial frustration into the system. The red and blue spins prefer to rotate in opposite directions due to circular anisotropy, but the coupling term tries to synchronize

doi.org/10.32388/9ZDJVU

them. This frustration is a key driver for the formation of complex, non-uniform phases like vortex/antivortex complexes, rather than simple global synchronization.

The system shows topological characteristics. The circular nature of the orientational degree of freedom facilitates the existence of defects characterized by integer winding numbers. The frustration induced by the c-spins and the dynamics in a 2D space enables the creation of stable defects associated with phase singularities. Indeed, composite patterns of topological orientational textures and spin-momentum locked loops emerge. These loops exhibit ballistic flow when local properties would predict high dissipation. The loops and the textures are not a separate phenomenon but form a composite topological state. These compound (texture + loop) patterns are non-local, self-organized (i.e., spread over distances much greater than the interaction length) vortex complexes, extremely robust to noise or perturbations. Such resilience, together with non-locality, dissipationless transport, and spin-momentum locking are distinctive hallmarks of a topological phase, and these patterns can be classified as topological dissipative structures. I have investigated the vortex complexes by means of illustrative movies and by numerically evaluating two collective parameters concerning spatial activity (the average kinetic energy) and phase synchronization (a modified Kuramoto order parameter). The system shows the coexistence of two phase transitions taking place for the same critical value of the control parameter: an “ordinary” symmetry-breaking phase transition associated with collective synchronization (as in the Kuramoto model), and a novel topological phase transition that activates the vortex complexes.

Increasing the system size leads to a notable increase in the complexity of the collective organization. In contrast to the single vortex that characterizes small systems, large systems exhibit a flexible, spin-momentum locked morphogenetic flow that percolates throughout the entire system. This flow creates a highly intricate and unpredictable dynamic for the texture-loop interaction. Although this phenomenon has been observed in previously published initial studies, the underlying mechanisms in these large-scale systems are still not fully understood and warrant further investigation.

The reasons for interest in the scenario put forward by this work are twofold. First is observing a novel topological phase in a classical dynamical system, unveiling a whole new class of non-equilibrium states. The robustness of the reported vortex complexes, along with their dissipationless transport and spin-momentum locking, are highly suggestive of a deeper theoretical underpinning.

Secondly, the emergence and self-organization of robust, non-local structures, which are sustained far from equilibrium by a dissipationless flow and structured by topological constraints, provide a new perspective on biological organization. Biological systems are fundamentally defined by emergent, self-

organized structures that operate far from thermodynamic equilibrium [21][22]. The emergence of flow and form from local interactions creating global (non-local) structures is a core principle of biological self-organization and reflects the scenario displayed in this work, which moreover provides a mechanism for dissipationless flow that enables the system to persist efficiently out-of-equilibrium, sustained by a minimal energy input. This efficiency is critical, as high dissipation releases—in physical systems—heat (entropy production), which would otherwise limit the structures' lifetime. Topological robustness provides resilience against noise and structural deterioration, granting the patterns a capacity for self-repair—another fundamental trait associated with living systems. Finally, the patterns show the emergence of a further, fundamental biological feature: *diversity*. This diversity is attributable, once again, to the topological character of those states, allowing for infinitely diverse, yet topologically equivalent, states composed of identical units, even under the same system conditions and parameters.

Far from being exhaustive, the present numerical study has only scratched the surface of a non-linear dynamical problem endowed with a surprising wealth of complex organizational dynamics.

Supplementary Materials

Movies S1, S2, S3, and S4.

Statements and Declarations

Funding

No funding was granted for the development of this work.

Conflicts of Interest

The author declares no conflicts of interest.

Author Contributions

A.S. is the sole author and is responsible for all aspects of the work presented in this manuscript, including conceptualization, methodology, simulations, data analysis, and writing.

Institutional Review Board Statement

Not applicable.

Informed Consent Statement

Not applicable.

Data Availability Statement

All data generated or analyzed during this study are included in this published article and its supplementary information files, Movies S1, S2, and S3.

Acknowledgments

The author thanks the University of Pavia for institutional support. The author is grateful for the personal dedication and tireless patience required to complete this work.

References

1. ^*Gompper G, Stone HA, Kurzthaler C, Saintillan D, Peruani F, Fedosov DA, Auth T, Cottin-Bizonne C, Ybert C, Clément E, Darnige T, Lindner A, Goldstein RE, Liebchen B, Binysh J, Souslov A, Isa L, di Leonardo R, Frangipane G, Gu H, Nelson BJ, Brauns F, Marchetti MC, Cichos F, Heuthe VL, Bechinger C, Korman A, Feinerman O, Cavagna A, Giardina I, Jeckel H, Drescher K (2025). "The 2025 Motile Active Matter Roadmap." J Phys Condens Matter. **37**:143501. doi:10.1088/1361-648x/adac98.*
2. ^*Bowick MJ, Fakhri N, Marchetti MC, Ramaswamy S (2022). "Symmetry, Thermodynamics, and Topology in Active Matter." Phys Rev X. **12**(1). doi:10.1103/physrevx.12.010501.*
3. ^*Vicsek T, Czirók A, Ben-Jacob E, Cohen I, Shochet O (1995). "Novel Type of Phase Transition in a System of Self-Driven Particles." Phys Rev Lett. **75**(6):1226–1229. doi:10.1103/physrevlett.75.1226.*
4. a, b*Edelsbrunner H, Letscher D, Zomorodian A (2002). "Topological Persistence and Simplification." Discrete Comput Geom. **28**(4):511–533.*
5. a, b*Shankar S, Souslov A, Bowick MJ, Marchetti MC, Vitelli V (2022). "Topological Active Matter." Nat Rev Phys. **4**(6):380–398. doi:10.1038/s42254-022-00445-3.*
6. ^*Shankar S, Bowick MJ, Marchetti MC (2017). "Topological Sound and Flocking on Curved Surfaces." Phys Rev X. **7**(3):031039. doi:10.1103/physrevx.7.031039.*
7. ^*Tubiana L, Alexander GP, Barbensi A, Buck D, Cartwright JHE, Chwastyk M, Cieplak M, Coluzza I, Čopar S, Craik DJ, Di Stefano M, Everaers R, Faísca PFN, Ferrari F, Giacometti A, Goundaroulis D, Haglund E, Hou YM, Ilieva N, Jackson SE, Japaridze A, Kaplan N, Klotz AR, Li H, Likos CN, Locatelli E, López-León T, Machon T, M*

*icheletti C, Michieletto D, Niemi A, Niemyska W, Niewieczerzal S, Nitti F, Orlandini E, Pasquali S, Perlinska A P, Podgornik R, Potestio R, Pugno NM, Ravnik M, Ricca R, Rohwer CM, Rosa A, Smrek J, Souslov A, Stasiak A, Steer D, Sułkowska J, Sułkowski P, Sumners DW, Svaneborg C, Szymczak P, Tarenzi T, Travasso R, Virnau P, V lassopoulos D, Ziherl P, Žumer S (2024). "Topology in Soft and Biological Matter." Phys Rep. **1075**:1–137. doi:10.1016/j.physrep.2024.04.002.*

8. ^*Saw TB, Doostmohammadi A, Nier V, Kocgozlu L, Thampi S, Toyama Y, Marcq P, Lim CT, Yeomans JM, Lad oux B (2017). "Topological Defects in Epithelia Govern Cell Death and Extrusion." Nature. **544**(7649):212–21 6. doi:10.1038/nature21718.*
9. ^*Saw TB, Doostmohammadi A, Nier V, Kocgozlu L, Thampi S, Toyama Y, Marcq P, Lim CT, Yeomans JM, Lad oux B (2017). "Topological Defects in Epithelia Govern Cell Death and Extrusion." Nature. **544**(7649):212–21 6. doi:10.1038/nature21718.*
10. ^*Maroudas-Sacks Y, Garion L, Shani-Zerbib L, Livshits A, Braun E, Keren K (2021). "Topological Defects in th e Nematic Order of Actin Fibers as Organization Centers of Hydra Morphogenesis." Nat Phys. **17**(2):251–259. doi:10.1038/s41567-020-01083-1.*
11. ^*Winfree AT (1967). "Biological Rhythms and the Behavior of Populations of Coupled Oscillators." J Theor B iol. **16**(1):15–42. doi:10.1016/0022-5193(67)90051-3.*
12. ^*Kuramoto Y (1976). "Cooperative Dynamics of a Nonlinear Differential Equation." In: Araki H, editor. Intern ational Symposium on Mathematical Problems in Theoretical Physics. Vol. 39. Springer-Verlag. p. 420–422.*
13. ^*Rouzaire Y, Levis D (2022). "Dynamics of Topological Defects in the Noisy Kuramoto Model in Two Dimen sions." Front Phys. **10**:Article 976515. doi:10.3389/fphy.2022.976515.*
14. ^*Acebrón JA, Bonilla LL, Pérez-Vicente CJ, Ritort F, Spigler R (2005). "The Kuramoto Model: A Simple Paradi gm for Synchronization Phenomena." Rev Mod Phys. **77**(1):137. doi:10.1103/RevModPhys.77.137.*
15. ^*O'Keeffe KP, Hong H, Strogatz SH (2017). "Oscillators That Sync and Swarm." Nat Commun. **8**(1):1504. doi:10.1038/s41467-017-01190-3.*
16. ^*Degond P, Diez A, Walczak A (2022). "Topological States and Continuum Model for Swarmalators Without Force Reciprocity." Anal Appl. **20**(06):1215–1270. doi:10.1142/s0219530522400073.*
17. a, b, c, d, e*Scirè A, Annovazzi-Lodi V (2023). "The Emergence of Dynamic Networks From Many Coupled Pol ar Oscillators: A Paradigm for Artificial Life." Theory Biosci. **142**(3):291–299. doi:10.1007/s12064-023-00401-4.*
18. a, b, c, d, e, f, g, h, i*Scirè A (2024). "Emergence and Criticality in Spatiotemporal Synchronization: The Comple mentarity Model." Artif Life. **30**(4):508–522. doi:10.1162/artl_a_00440.*

19. a, b *Scirè A, Annovazzi-Lodi V (2017). "Self-Organization in a Diversity Induced Thermodynamics." PLoS ON E. **12**(12):e0188753. doi:10.1371/journal.pone.0188753.*

20. ^ *Adler R (1946). "A Study of Locking Phenomena in Oscillators." Proc IRE. **34**(6):351–357.*

21. a, b *Prigogine I, Stengers I (1984). Order Out of Chaos: Man's New Dialogue With Nature. New York: Bantam Books.*

22. a, b *Camazine S, Deneubourg JL, Franks NR, Sneyd J, Theraulaz G, Bonabeau E (2003). Self-Organization in B iological Systems. Princeton: Princeton University Press.*

Declarations

Funding: No specific funding was received for this work.

Potential competing interests: No potential competing interests to declare.